THE ASTROPHYSICAL JOURNAL, 555:829–833, 2001 July 10
© 2001. The American Astronomical Society. All rights reserved. Printed in U.S.A.

BIZARRE HARD X-RAY OUTBURSTS OF CYGNUS X-1

BORIS E. STERN,[1,2] ANDREI M. BELOBORODOV,[1] AND JURI POUTANEN
Stockholm Observatory, SE-133 36 Saltsjöbaden, Sweden; juri@astro.su.se
Received 2000 May 18; accepted 2001 March 6

ABSTRACT

Very high activity in Cygnus X-1 during 1999 April 19–21 was recorded by the BATSE Large Area Detectors on board the *Compton Gamma Ray Observatory*. The peak luminosity was an order of magnitude higher than the normal luminosity of Cyg X-1. This fact can be critical for models of the hard state of Cyg X-1. The longest outburst lasted $\sim$1000 s and demonstrated very unusual temporal and spectral behavior, which indicates the presence of two emission components. One component is relatively soft (with a cutoff below $\sim$100 keV) and highly variable, while the other is hard (extending above 100 keV) with much slower variability.

Subject headings: accretion, accretion disks — gamma rays: observations — stars: individual (Cygnus X-1)

1. INTRODUCTION

Cygnus X-1 is a persistent X-ray source believed to be powered by accretion onto a black hole from a massive companion. Cyg X-1 spends most of the time in the hard state and sometimes switches to the soft state (see, e.g., Liang & Nolan 1984; Zhang et al. 1997; Poutanen 1998; Gierliński et al. 1999). The X-ray luminosity above $\sim$2 keV is estimated to be about 3×10^{37} ergs s^{-1} (Gierliński et al. 1997), assuming a distance to the source $D = 2$ kpc (Massey, Johnson, & DeGioia-Eastwood 1995; Malysheva 1997).

The variability of Cyg X-1 has been extensively studied with various instruments (see, e.g., Ling et al. 1987; Gilfanov et al. 1995; Phlips et al. 1996; Kuznetsov et al. 1997; Paciesas et al. 1997; Wen et al. 1999; Brocksopp et al. 1999; Bałucińska-Church et al. 2000). These studies have demonstrated the stability of the hard state of Cyg X-1. The photon flux above 50 keV is normally $\sim$0.1 photons cm^{-2} s^{-1} with variations by a factor of 2.

In this paper we analyze the period of the unusually strong hard X-ray activity of Cyg X-1 on 1999 April 21. Two strong outbursts activated the onboard trigger of the Burst and Transient Source Experiment (BATSE; Fishman et al. 1989) on the *Compton Gamma Ray Observatory* (*CGRO*). We analyze the temporal structure of the outbursts in the Large Area Detector (LAD) energy channels 1–4, estimate the peak luminosity of Cyg X-1, and discuss possible implications for theoretical models of accretion in this object.

2. THE OUTBURSTS

The unusual activity of Cyg X-1 can be traced back to 1999 April 19 (TJD 11,287). Two events recorded on April 19 were found in the BATSE data during a search for non-triggered gamma-ray bursts (GRBs) (Stern et al. 1999, 2000). The best-fit locations were within 4°–5° from Cyg X-1 (1 σ errors exceeded 10° for those events). We use the location procedure described in Stern et al. (2001), which is similar to that used for GRB location by Pendleton et al. (1999). The estimated peak fluxes above 50 keV were about 0.3 and 0.5 photons cm^{-2} s^{-1}, which is high compared with the normal flux from Cyg X-1. On April 20, BATSE detectors were triggered by another event with right ascension $\alpha = 305\overset{\circ}{.}1$ and declination $\delta = 26\overset{\circ}{.}2$ (BATSE estimate; note also that this event is identified as a GRB in the BATSE database). Again, the location was close to Cyg X-1 (slightly beyond the 1 σ error circle).[3] The peak flux of this event was about 0.5 photons cm^{-2} s^{-1}.

On April 21, the two brightest outbursts occurred with an interval of $\sim$2.5 hr. Between and after the two outbursts, Cyg X-1 demonstrated nothing unusual, being in the hard state with normal luminosity. A summary of all five events is given in Table 1.

We concentrate on the two brightest events on April 21 (the last two rows in Table 1). The location of both events coincides with the location of Cyg X-1 with 2° accuracy. In principle, they might be accidental projections of GRBs on Cyg X-1. The probability that one of $\sim 10^3$ detected GRBs with comparable brightness will appear within 2° from Cyg X-1 is about 0.3. However, the probability of appearance of two such GRBs from the same location within 2.5 hr is low, $\sim 10^{-5}$. In addition, the long duration of the events, $\sim 10^3$ s, is very unusual for GRBs. One concludes that the events are outbursts of Cyg X-1.

2.1. *Outburst 11289c*

The first outburst on April 21 has similar light curves in LAD energy channels 1–3 (Fig. 1, *top*). The signal in channel 4 (above 300 keV) was low—practically undetectable. The signal was cut off by Earth occultation at $\approx$55.23 ks. We model the background during the outburst using a linear fit, extrapolating the background after the occultation.

In order to obtain the photon and energy fluxes, we fitted the signal count rate in the three energy channels using the detector response matrix computed with the code of Pendleton (see Pendleton et al. 1999 and references therein). An exponentially cut off power law is assumed as a spectral hypothesis. The photon and energy fluxes are then obtained by integrating the best-fitting spectrum in the proper energy band. The error is estimated to be about 15%. (Note that the overall systematic error in the BATSE flux normalization may be about 20%; see, e.g., Much et al. 1996.)

[1] Also Astro Space Center, Lebedev Physical Institute, Russian Academy of Sciences, Profsoyuznaya 84/32, 117810 Moscow, Russia.

[2] Also Institute for Nuclear Research, Russian Academy of Sciences, 117312 Moscow, Russia.

[3] The coordinates of Cyg X-1 are $\alpha = 299\overset{\circ}{.}5$ and $\delta = 35\overset{\circ}{.}2$.

TABLE 1

SUMMARY OF OUTBURSTS: 1999 APRIL 19–21

ST2000[a]	No.[b]	Time[c] (s)	α^d (deg)	δ^d (deg)	1 σ^d (deg)
11287a.....	...	16,816	297.8	38.2	18.4
11287b.....	...	18,071	296.6	38.0	12.9
11288e.....	7523	83,437	305.6	27.6	6.0
11289c.....	7524	54,530	299.9	34.4	2.4
11289e.....	7525	63,100	298.4	35.2	1.2

[a] Name in the catalog of Stern et al. 1999, consisting of TJD and a letter.
[b] BATSE trigger number.
[c] Time of day.
[d] The best-fit location and its 1 σ error.

The peak flux in 50–300 keV band (channels 2–3) is about 1.1 photons cm^{-2} s^{-1}, which is $\sim$10 times higher than the normal flux from Cyg X-1. The flux averaged over 100 s (54.55–54.65 ks interval) is 0.75 photons cm^{-2} s^{-1}. The peak luminosity above 30 keV exceeds 10^{38} ergs s^{-1} (see Table 2 for details). Note that the strong increase in the luminosity was not accompanied by crucial changes in the spectrum. At least, the hardness ratios during the outburst remained similar to the normal hard state of Cyg X-1 (see § 3).

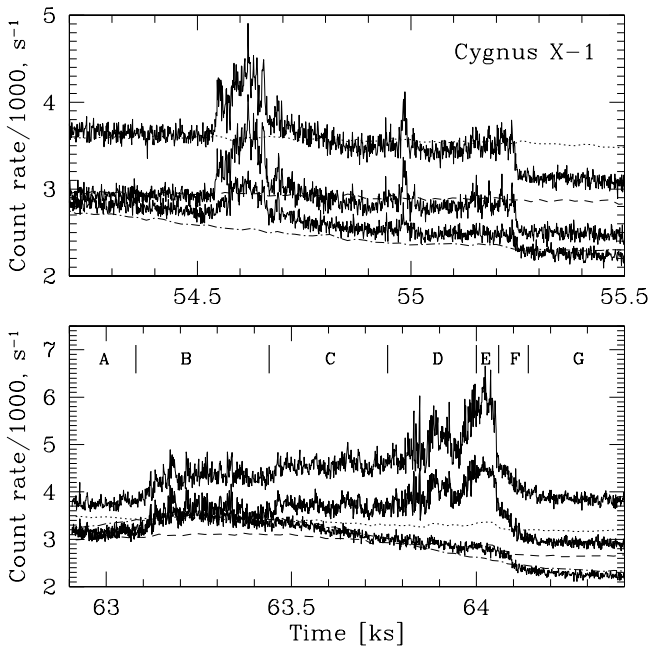

FIG. 1.—Count rate during the two outbursts of Cyg X-1 on 1999 April 21 (TJD 11,289) in LAD energy channels 1–3. The count rate is summed over two detectors closest to the line of sight to Cyg X-1. Count rates are higher in softer channels. Dotted, dashed, and dot-dashed curves show the background in channels 1, 2, and 3, respectively, as seen by two detectors looking away from Cyg X-1.

TABLE 2

PEAK FLUXES AND LUMINOSITIES

Outburst	$F_{>50}$[a]	$F_{>30}$[b]	$L^c_{>50}$	$L^d_{>30}$
11289c.....	1.1	2.4	0.75×10^{38}	1.2×10^{38}
11289e.....	1.3	3.9	0.8×10^{38}	1.6×10^{38}

[a] Peak flux (photons cm^{-2} s^{-1}) above 50 keV.
[b] Peak flux above 30 keV.
[c] Peak luminosity (ergs s^{-1}) above 50 keV (assuming distance $D = 2$ kpc).
[d] Peak luminosity above 30 keV.

2.2. *Outburst 11289e*

The second outburst on April 21 was detected $\sim$8 ks after the first outburst (see Fig. 1, *bottom*). Unfortunately, there is a gap in the data at the time when Cyg X-1 rose above the horizon ($\sim$62.8 ks). The data records start at $\approx$62.9 ks. Note that there was no occultation of Cyg X-1 at the end of the outburst. The sharp falloff in the light curves in each channel is the intrinsic behavior of the source. It allows one to estimate the peak flux and luminosity of the outburst, which we give in Table 2. The corresponding luminosities averaged over interval E (see Fig. 1) are 20% smaller than the peak values.

The ionospheric background showed smooth latitude variations during the outburst (see Fig. 1, *bottom*) on the timescale of order 1 ks. The background level is different in different detectors; therefore, it is difficult to exactly extract the signal seen in the detectors looking at Cyg X-1. The signal uncertainty caused by the background variations is of order 20%.

One can get a good location fit for the signal by analyzing the variable part of the light curve. At a given time interval, we fit the light curve by a linear function and take it as a "reference" level. (It thus includes both the background and the linear part of the true signal.) We then take the difference between the count rate (at this or another interval) and the reference level as a "signal." The location fits demonstrate that almost all the variable part of the signal comes from the direction of Cyg X-1 with $\sim$5° accuracy at the time intervals A–F marked in Figure 1 (see Table 3). The residual signal can be fitted by 200–400 s long linear fragments with a good χ^2 (rows 1–3 in Table 3). This means that no fraction of the variable signal can be mimicked by magnetospheric phenomena such as particle precipitation, which either produces a diffuse flux of photons or can be a localized source at some distance from the spacecraft. In the first case, the location fit is so poor that the residual χ^2 is comparable to the initial one, and in the second case, one observes a fast change in the direction of the source due to the satellite's motion. In our case, the satellite moved $\sim$6000 km between intervals B and E, while the source's position on the sky did not change.

TABLE 3

LOCATION FITS FOR DIFFERENT TIME INTERVALS

Signal[a]	Reference[b]	Channel	α^c (deg)	δ^c (deg)	1 σ^c (deg)	$\chi^2_0/\chi^{2\,d}_r$
B	B	2+3	302.1	37.1	6.6	11.4/0.93
D+E...	D+E	1	302.3	38.4	2.0	34.0/1.13
		2+3	301.3	40.2	6.0	16.9/1.05
	G	2+3	298.4	35.2	1.2	447/10.8
E	E	1	303.9	40.1	4.9	15.3/0.90
E+F ...	G	3	298.8	33.5	2.1	64.4/2.35
F	G	2+3	302.4	40.3	4.1	51.0/1.66

[a] The time interval in which the location fit is done for the residuals after subtracting a linear ("reference") function from the count rate.
[b] The interval at which the linear reference function was fitted.
[c] The best-fit location and its 1 σ error.
[d] Here χ^2_0 and χ^2_r are χ^2 per degree of freedom for the count rate relative to the reference level and for the residual signal after the location fit, respectively.

TABLE 4

CHARACTERISTICS OF COUNT RATE VARIABILITY

Interval	rms_1	rms_2	rms_3	c_{23}	fhr_{21}
A.....	97	109	70	0.63 ± 0.09	1.12 ± 0.06
B.....	300	316	169	0.92 ± 0.02	1.05 ± 0.02
C.....	211	213	96	0.77 ± 0.05	1.01 ± 0.03
D	499	370	100	0.71 ± 0.04	0.74 ± 0.01
E.....	568	286	90	0.15 ± 0.07	0.50 ± 0.02
F.....	109	196	106	0.92 ± 0.07	1.32 ± 0.10

NOTE—The 1 σ errors of c_{23} and fhr_{21} are of Poisson nature; they are estimated with the bootstrap method. The measured hardness ratios are not affected by the background uncertainty, because they are based on the signal dispersion in a narrow time interval where the background is almost linear.

While the first April 21 outburst is unusual only for its strength, the second one is even more surprising. The behavior of the light curve in different energy channels suggests the presence of two independent emission components. The first (highly variable) component dominates the signal in channels 1 and 2, and the second component (with low amplitude of variability) dominates the signal in channel 3. The soft component terminated at 64.05 ks, and then one observes only the hard component in the three channels. Unfortunately, the spectral data for this outburst were lost, which prevented our confirming the two components by spectral analysis.

Since we cannot accurately separate the signal from the background, we study the outburst using the strong non-Poisson variability produced by the signal in the count rate. In each time interval, A–F, we compute the root mean square (rms) of the signal variations, S_i, around the linear fits (i = 1, 2, 3 is the channel number). We then compute the "fluctuation hardness ratio" (fhr), which is the ratio of the rms in different channels. The rms (with subtracted Poisson component) and $fhr_{21} \equiv rms_2/rms_1$ are given in Table 4. Assuming the rms to be roughly proportional to the average level of the signal, the fhr may give an estimate for the true hardness ratio. The decrease of fhr_{21} as the outburst progresses indicates that the variable component gets softer.

We then compute the cross-correlation coefficient between channels 2 and 3, $c_{23} \equiv (\langle S_2 S_3 \rangle - \langle S_2 \rangle \langle S_3 \rangle)/rms_2\, rms_3$ (see Table 4). The cross-correlation decreases during the outbursts and becomes very low in interval E. It confirms that the soft component gets so soft that it practically does not contribute to the signal in channel 3. In interval F, the cross-correlation is high, confirming that the soft component has disappeared and that we see only the second (hard) component in all three channels. The luminosities of the soft and hard components can be roughly estimated from the steplike cutoffs at 64.05 and 64.1 ks, respectively. The average luminosity of Cyg X-1 in time interval E above 50 keV (30 keV) is $L_{>50} \sim 2.5 \times 10^{37}$ ergs s^{-1} ($L_{>30} \sim 7.0 \times 10^{37}$ ergs s^{-1}) in the soft component and $L_{>50} \sim 4.0 \times 10^{37}$ ergs s^{-1} ($L_{>30} \sim 5.5 \times 10^{37}$ ergs s^{-1}) in the hard component.

3. COMPARISON WITH THE NORMAL HARD STATE OF CYGNUS X-1

The normal hard state of Cyg X-1 was studied using the Earth occultations that occur on each orbit of the *CGRO*. The step in the light curve at the moment of occultation shows the amplitude of the signal from Cyg X-1 in each energy channel. The study of Cyg X-1 with this method was done by Ling et al. (1997) and Paciesas et al. (1997). We performed a similar analysis for ~60 occultations and evaluated the flux from Cyg X-1 and the hardness ratio hr_{32} (ratio of the signal count rates in channels 3 and 2) for each occultation. The results are shown in Figure 2. The observed large dispersion in the hardness ratio may be caused by the measurement errors rather than the intrinsic variability of Cyg X-1. To estimate the errors, we performed a similar analysis of 80 occultations of the Crab nebula, which is known to be a steady source. We found $hr_{32} = 0.66 \pm 0.13$ and a count rate 316 ± 110, where the errors represent the standard deviations. The major cause of the errors is the uncertainty in the changing background (to have good statistics, one has to fit the signal on a relatively long period, ~100 s, before and after the occultation, and the background curvature plays a role). One should note that the error in the hardness ratio of Cyg X-1 is likely to be smaller than that for the Crab, since its flux is larger. In the outbursts, these errors are even smaller.

For comparison we also show the estimates of the flux and hardness ratio for the two April 21 outbursts. Note that outburst 11289c and interval F of outburst 11289e have hardness ratios similar to the normal hard state. Interval E of outburst 11289e is significantly softer.

The presence of two emission components (soft, highly variable, and hard, with lower variability) in outburst 11289e is intriguing. Are they present in the normal state of Cyg X-1? In the sample of 63 occultations we found that the fractional rms of the count rate (i.e., the ratio of the rms to

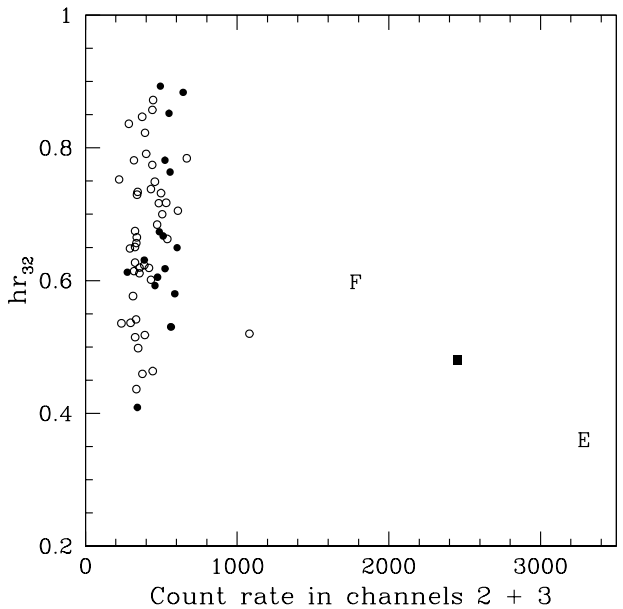

FIG. 2.—Hardness ratio, hr_{32}, of signal count rates in channels 3 and 2 vs. count rate in channels 2+3, as measured in all detectors (note the difference from Fig. 1, where the count rate is given only for two detectors). Open circles show a sample of occultations in the period TJD 8,600–8,700; filled circles show the same in the period TJD 9,990–10,000. Cyg X-1 was in the normal hard state with relatively high brightness in both periods. The dispersion in hr_{32} may be caused by measurement errors (see text). The square corresponds to the first outburst on April 21 (between 54.55 and 54.65 ks). Labels F and E represent the second outburst on April 21 in time intervals F and E, respectively. (The signal was roughly estimated by subtracting the level of the count rate in interval G.)

the mean count rate) in channel 2 was higher than that in channel 3 in 47 cases. This indicates higher variability in channel 2 (the probability of such an accidental excess is 0.5×10^{-4}). The decreasing of the variability with energy was also observed in the 2–40 keV band (Nowak et al. 1999; Revnivtsev et al. 2000). These facts are consistent with the presence of a hard component with a low variability, although this interpretation is not unique. Note also that Gierliński et al. (1997) obtained the best fit to the broadband X-ray spectrum of Cyg X-1 with two thermal Comptonization components of different temperatures.

4. DISCUSSION

The hard state of Cyg X-1 has been a puzzle since its discovery. The standard accretion disk model (Shakura & Sunyaev 1973) was not able to explain the X-ray spectrum, and two modifications of the model were suggested: a two-temperature hot disk and an active corona atop the standard disk (see Beloborodov 1999a for a recent review).

The advective hot disk models (e.g., Esin et al. 1998) are consistent with the observed spectrum and luminosity of Cyg X-1 if the accretion rate has a specific value of $\dot{M} \approx \dot{M}_* \approx 10\alpha^2 L_E/c^2$ and the viscosity parameter $\alpha \approx 0.2$–0.3. Here $L_E = 4\pi cGMm_p/\sigma_T = 1.3 \times 10^{39}[M/(10\ M_\odot)]$ ergs s^{-1} is the Eddington luminosity. Small variations in the accretion rate, $\Delta\dot{M}/\dot{M} \sim 10\%$, were predicted to destroy the hard state (Esin et al. 1998; but see also Zdziarski 1998). By contrast, the luminosity of Cyg X-1 is known to vary by a factor of 2 without substantial changes in the spectral shape (e.g., Paciesas et al. 1997; Gierliński et al. 1997). Such fluctuations already challenged the model, and the hard outbursts analyzed in this paper are even more difficult to explain. The model would work only by assuming a specific dependence $\alpha \propto \dot{M}^{1/2}$ that keeps $\dot{M} \approx \dot{M}_*$; α should then be about unity at the peak of the outburst.

In the context of the disk corona model, the outbursts can be interpreted as an enhanced coronal activity of the accretion disk. In this model, the X-ray spectral slope is controlled by one parameter, the feedback factor due to X-ray reprocessing by the disk. The hard-state spectrum of Cyg X-1 is well explained if the coronal plasma is ejected away from the disk with a mildly relativistic velocity $\beta = v/c \sim 0.3$ (Beloborodov 1999b; Malzac, Beloborodov, & Poutanen 2001). Alternatively, the observed emission may be produced by a static corona atop a strongly ionized disk (e.g., Ross, Fabian, & Young 1999; Nayakshin 1999). The corona becomes $e^{\pm}$ dominated at high luminosities and its temperature decreases (e.g., Svensson 1984; Stern et al. 1995; Poutanen & Svensson 1996). Pair creation may cause the shift of the spectral break in outburst 11289e to smaller energies.

Cyg X-1 is a massive X-ray binary and it may be fed mainly by the donor wind. Then the pattern of accretion could change completely compared with the standard viscous α-disk or its modifications. The captured wind matter has a low angular momentum, which is just about critical for disk formation (Illarionov & Sunyaev 1975). Under such conditions, a small-scale inviscid disk forms that accretes supersonically (Beloborodov & Illarionov 2001). The disk forms in the ringlike caustic of the accretion flow, where energy is liberated in the inelastic collision of gas streams. A Comptonized power-law spectrum is then emitted with a standard break at $\sim$100 keV and has the appearance of a normal hard state of Cyg X-1.

The two-component emission in outburst 11289e probably requires a two-zone emission model. For instance, the soft component may be associated with a variable coronal emission atop the disk, and the hard component with an inner relativistic jet. A corona jet model was recently proposed by Brocksopp et al. (1999) based on correlations between the X-rays and the radio emission observed in Cyg X-1. The 1999 April outbursts were, however, too short to have a significant impact on the flux in radio, and no substantial changes were detected (R. Fender & G. Pooley 2000, private communication). In the context of the wind-fed accretion model, the two-component emission can naturally appear if a viscous accretion disk coexists with an inner inviscid disk.

In conclusion, the 1999 April 21 outbursts are the brightest events detected from Cyg X-1 by BATSE during 9 years of its operation. The hard X-ray luminosity above 30 keV was in excess of 10^{38} ergs s^{-1}. Unfortunately, there are no simultaneous observations in the soft X-rays, so one can only guess what the total luminosity was. The large luminosity and unusual spectral behavior challenge the theoretical models of accretion in Cyg X-1.

We thank Rob Fender, Guy Pooley, and Jerry Bonnell for useful discussions. We are grateful to Rob Preece and Geoff Pendleton for providing the code for computing the detector response matrix, and to an anonymous referee for useful comments that significantly improved the paper. This research has made use of data obtained through the High Energy Astrophysics Science Archive Research Center Online Service provided by the NASA Goddard Space Flight Center. This work was supported by the Swedish Natural Science Research Council, the Swedish Royal Academy of Sciences, the Wenner-Gren Foundation for Scientific Research, the Anna-Greta and Holger Crafoord Fund, and RFBR grant 00-02-16135.

REFERENCES

Bałucińska-Church, M., Church, M. J., Charles, P. A., Nagase, F., LaSala, J., & Barnard, R. 2000, MNRAS, 311, 861
Beloborodov, A. M. 1999a, in ASP Conf. Ser. 161, High Energy Processes in Accreting Black Holes, ed. J. Poutanen, & R. Svensson (San Francisco: ASP), 295
———. 1999b, ApJ, 510, L123
Beloborodov, A. M., & Illarionov, A. F. 2001, MNRAS, 323, 167
Brocksopp, C., Fender, R. P., Larionov, V., Lyuty, V. M., Tarasov, A. E., Pooley, G. G., Paciesas, W. S., & Roche, P. 1999, MNRAS, 309, 1063
Esin, A. A., Narayan, R., Cui, W., Grove, J. E., & Zhang, S.-N. 1998, ApJ, 505, 854
Fishman, G. J., et al. 1989, in Proc. Gamma Ray Observatory Science Workshop, ed. W. N. Johnson (Greenbelt, MD: GSFC), 3-47
Gierliński, M., Zdziarski, A. A., Done, C., Johnson, W. N., Ebisawa, K., Ueda, Y., Haardt, F., & Phlips, B. F. 1997, MNRAS, 288, 958
Gierliński, M., Zdziarski, A. A., Poutanen, J., Coppi, P. S., Ebisawa, K., & Johnson, W. N. 1999, MNRAS, 309, 496
Gilfanov, M., et al. 1995, in Lives of the Neutron Stars, ed. M. A. Alpar, U. Kízíloğlu, & J. van Paradijs (NATO ASI Ser. C, 450) (Dordrecht: Kluwer), 331
Illarionov, A. F., & Sunyaev, R. A. 1975, A&A, 39, 185
Kuznetsov, S., et al. 1997, MNRAS, 292, 651
Liang, E. P., & Nolan, P. L. 1984, Space Sci. Rev., 38, 353
Ling, J. C., Mahoney, W. A., Wheaton, W. A., & Jacobson, A. S. 1987, ApJ, 321, L117
Ling, J. C., et al. 1997, ApJ, 484, 375

Malysheva, L. K. 1997, AZh Pisma, 23, 667 (English transl. Astron. Lett., 23, 585)
Malzac, J., Beloborodov, A. M., & Poutanen, J. 2001, MNRAS, in press
Massey, P., Johnson, K. E., & DeGioia-Eastwood, K. 1995, ApJ, 454, 151
Much, R., et al. 1996, A&AS, 120, C703
Nayakshin, S. 1999, in ASP Conf. Ser. 162, Quasars and Cosmology, ed. G. Ferland, & J. Baldwin (San Francisco: ASP), 87
Nowak, M. A., Vaughan, B. A., Wilms, J., Dove, J. B., & Begelman, M. C. 1999, ApJ, 510, 874
Paciesas, W. S., Robinson, C. R., McCollough, M. L., Zhang, S. N., Harmon, B. A., Wilson, C. A. 1997, in AIP Conf. Proc. 410, Proc. Fourth Compton Symposium, ed. C. D. Dermer, M. S. Strickman, & J. M. Kurfess (New York: AIP), 834
Pendleton, J. N., et al. 1999, ApJ, 512, 362
Phlips, B. F., et al. 1996, ApJ, 465, 907
Poutanen, J. 1998, in Theory of Black Hole Accretion Disks, ed. M. A. Abramowicz, G. Björnsson, & J. E. Pringle (Cambridge: Cambridge Univ. Press), 100
Poutanen, J., & Svensson, R. 1996, ApJ, 470, 249
Revnivtsev, M. G., Borozdin, K. N., Priedhorsky, W. C., & Vikhlinin, A. 2000, ApJ, 530, 955
Ross, R. R., Fabian, A. C., & Young, A. J. 1999, MNRAS, 306, 461
Shakura, N. I., & Sunyaev, R. A. 1973, A&A, 24, 337
Stern, B. E., Poutanen, J., Svensson, R., Sikora, M., & Begelman, M. C. 1995, ApJ, 449, L13
Stern, B. E., Tikhomirova, Ya., Kompaneets, D., Stepanov, M., Berezhnoy, A., & Svensson, R. 1999, in ASP Conf. Ser. 190, Gamma-Ray Bursts: The First Three Minutes, ed. J. Poutanen, & R. Svensson (San Francisco: ASP), 253
Stern, B. E., Tikhomirova, Ya., Kompaneets, D., Svensson, R., & Poutanen, J. 2001, ApJ, in press
Stern, B. E., Tikhomirova, Ya., Stepanov, M., Kompaneets, D., Berezhnoy, A., & Svensson, R. 2000, ApJ, 540, L21
Svensson, R. 1984, MNRAS, 209, 175
Wen, L., Cui, W., Levine, A. M., & Bradt, H. V. 1999, ApJ, 525, 968
Zdziarski, A. A. 1998, MNRAS, 296, L51
Zhang, S. N., Cui, W., Harmon, B. A., Paciesas, W. S., Remillard, R. E., & van Paradjis, J. 1997, ApJ, 477, L95